

SAND97-3175C  
SAND-97-3175C  
RECEIVED

## IMPROVED ACCURACY FOR LOW-COST SOLAR IRRADIANCE SENSORS

David L. King, William E. Boyson, and Barry R. Hansen  
Sandia National Laboratories  
Albuquerque, New Mexico, USA  
<http://www.sandia.gov/pv/>

JUL 07 1998  
OSTI  
CONF-980735--

**ABSTRACT:** Accurate measurements of broadband (full spectrum) solar irradiance are fundamental to the successful implementation of solar power systems, both photovoltaic and solar thermal. Historically, acceptable measurement accuracy has been achieved using expensive thermopile-based pyranometers and pyrheliometers. The measurement limitations and sensitivities of these expensive radiometers are a topic that has been addressed elsewhere. This paper demonstrates how to achieve acceptable accuracy ( $\pm 3\%$ ) in irradiance measurements using sensors costing less than one-tenth that of typical thermopile devices. The low-cost devices use either silicon photodiodes or photovoltaic cells as sensors, and in addition to low-cost, have several operational advantages.

Keywords: Pyranometer-1: PV Module-2: Reference Cell-3

### 1. INTRODUCTION

Thousands of photovoltaic systems, large and small, are now being installed worldwide. As a result, there is a growing demand for inexpensive devices for accurately monitoring the solar irradiance. Most often, the total (global) solar irradiance is the desired measurement. Occasionally, the direct normal (beam) irradiance is required. For most system applications, reasonable accuracy ( $\pm 5\%$ ) at low cost (~200 \$US) is usually preferable to high accuracy ( $\pm 2\%$ ) at high cost (~2000 \$US). As a result, silicon photodiode pyranometers manufactured by companies such as LI-COR Incorporated [1] and Kipp & Zonen [2] are now commonly used for solar resource measurements and photovoltaic system monitoring. One manufacturer alone (LI-COR) has sold over 31,000 of their low-cost silicon photodiode-based pyranometers. Commercial solar cells have also been packaged in a variety of ways to serve as solar irradiance sensors. Traditional photovoltaic reference cells [3] have been used for many years in test laboratories, occasionally for field applications. Irradiance sensors designed for easy temperature compensation have been produced using two solar cells and standard module lamination procedures by the European Solar Test Installation (ESTI) [4], and by module manufacturers such as AstroPower Incorporated [5]. Small commercial photovoltaic modules have also frequently been used for measuring the solar irradiance.

These photovoltaic-based devices have typically provided a reasonable method for measuring the integrated daily solar irradiance (radiation). However, when used to measure the instantaneous broadband solar irradiance, their accuracy has been less than desired. Their inaccuracy has been due to errors introduced by systematic, time-of-day dependent, variations in the solar spectrum, solar angle-of-incidence, and operating temperature. A method was described in our previous work for obtaining empirical relationships that compensate for these systematic

errors [6, 7]. The purpose of this paper is to demonstrate the improvement achieved by applying these corrections. The corrections result in measurement accuracy comparable to more expensive instruments, for both global and direct normal solar irradiance.

### 2. LOW-COST IRRADIANCE SENSORS

Fig. 1 illustrates a few of the low-cost sensors evaluated in our work. The low-cost devices illustrated include a LI-COR LI-200SA silicon-photodiode pyranometer, a LI-COR LI-200SA fitted with a baffled plastic (PVC) collimator, an ESTI Sensor using two crystalline silicon cells, a two-cell mini-module fabricated by AstroPower using their Silicon-Film™ cell technology, and a common silicon reference cell. For comparison, an Eppley PSP pyranometer [8] is also shown in Fig. 1. For photovoltaic-based devices, empirical "corrections" were developed to compensate for the systematic influences mentioned. Controlled tests were then conducted to compare irradiance measurements, with and without the corrections, to the measurements obtained using carefully calibrated Eppley thermopile-based instruments.

### 3. SOLAR SPECTRAL INFLUENCE

Compensation for the influence of the time-of-day dependent solar spectrum was achieved by using an empirically determined function [7]. This empirical function,  $f_1(AM_a)$ , related solar spectral variations to the absolute air mass ( $AM_a$ ). "Air mass" is the term used to describe the path length that sunlight traverses through the atmosphere before reaching the ground. When adjustment is made for the altitude of the site, it is called the "absolute" air mass.  $AM_a$  is readily calculated knowing the zenith angle of the sun and the site altitude [7]. At sea level,  $AM_a=1$  with the sun directly overhead,  $AM_a=1.5$  when the sun's zenith angle is 48 degrees, and  $AM_a$  of about 10 at sunrise and

Sandia is a multiprogram laboratory operated by Sandia Corporation, a Lockheed Martin Company, for the U. S. Department of Energy under contract DE-AC04-94AL85000.

DISTRIBUTION OF THIS DOCUMENT IS UNLIMITED

MASTER

## **DISCLAIMER**

This report was prepared as an account of work sponsored by an agency of the United States Government. Neither the United States Government nor any agency thereof, nor any of their employees, makes any warranty, express or implied, or assumes any legal liability or responsibility for the accuracy, completeness, or usefulness of any information, apparatus, product, or process disclosed, or represents that its use would not infringe privately owned rights. Reference herein to any specific commercial product, process, or service by trade name, trademark, manufacturer, or otherwise does not necessarily constitute or imply its endorsement, recommendation, or favoring by the United States Government or any agency thereof. The views and opinions of authors expressed herein do not necessarily state or reflect those of the United States Government or any agency thereof.

## **DISCLAIMER**

**Portions of this document may be illegible electronic image products. Images are produced from the best available original document.**

sunset. As  $AM_a$  increases, the spectrum of the sun shifts to longer wavelengths, becoming more "red."

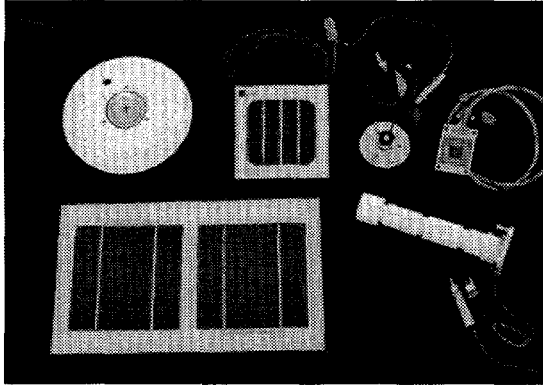


**Fig. 1:** Solar irradiance sensors, clockwise from upper left: Eppley PSP pyranometer, ESTI Sensor, LI-COR LI-200SA silicon-photodiode pyranometer, silicon reference cell, LI-COR LI-200SA with collimator, and AstroPower minimodule.

The concept of the empirical  $f_1(AM_a)$  function can be understood by examining the standard ASTM method for calculating a "spectral mismatch correction" [9]. The test procedure used for determining  $f_1(AM_a)$  basically provides a method for measuring a continuously varying spectral correction, referenced to one of two standardized spectra. These two solar spectra have been standardized by ASTM as references for the  $AM_a=1.5$  condition, one for the direct normal spectrum and one for the global spectrum [10, 11]. The  $f_1(AM_a)$  function is normalized to a value of one at  $AM_a=1.5$ , using one of these two standardized spectra.

Fig. 2 shows the  $f_1(AM_a)$  functions measured for the low-cost irradiance sensors, for clear-sky test conditions in Albuquerque, NM. For clear-sky conditions, experience has also shown that these empirically determined relationships have wide applicability to different sites. The solar spectral variation over the day resulted in an effect on the normalized response (short-circuit current) that was characteristic for each device. The magnitude of the spectral effect was directly related to the spectral response characteristics of the device. For instance, the 10% change in response for the LI-COR pyranometer from  $AM_a=1$  to  $AM_a=5$  resulted from a negligible spectral response at "blue" wavelengths ( $< 400$  nm) and good "red" response ( $> 900$  nm). The LI-COR equipped with a collimating tube showed slightly less spectral influence over the day because the spectral distribution of the direct normal irradiance differs from the total (global) normal spectrum.

#### 4. SOLAR ANGLE-OF-INCIDENCE

The irradiance sensor's response to the direct (beam) irradiance component is influenced by the cosine of the solar angle-of-incidence (AOI), and by the optical characteristics of its front surface. The response of the sensor to diffuse irradiance can be assumed to

have no dependence on angle-of-incidence. The algorithms for calculating AOI are documented elsewhere [12]. The optical influence of the front surface, which could be a flat- or domed-glass cover or a translucent diffuser, can be described by another empirically determined function,  $f_2(AOI)$ . An outdoor test procedure for determining the  $f_2(AOI)$  function is documented elsewhere [7].

Fig. 3 illustrates the relative response of the irradiance sensors versus the solar angle-of-incidence. For comparison, test results for a well-behaved Eppley PSP pyranometer are also shown. For clarity, measured data points for two of the devices are shown, and in other cases only the polynomial fit to measured values. The sensors with a planar glass front surface have a stronger sensitivity to AOI, for angles greater than 60 degrees. To some degree, the stronger sensitivity is offset by the observation that the planar devices have more repeatable behavior, device to device, than many commercial pyranometers. Users should recognize that all pyranometers are subject to significant measurement errors at high AOI due to mechanical misalignment. For instance at  $AOI=70$  degrees, mounting a pyranometer only 1 degree different from the plane of a photovoltaic array will result in a 5% error in measured irradiance.

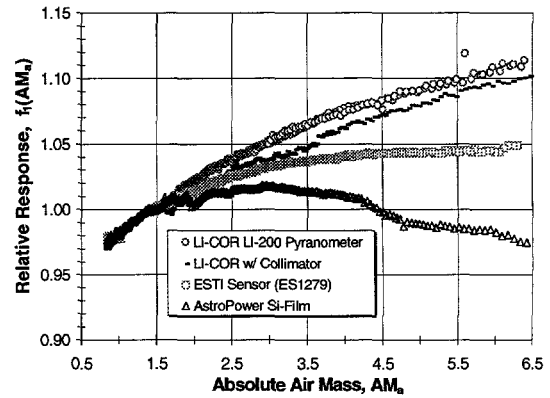


**Fig. 2:** Influence of solar spectral variation ( $AM_a$ ) on response (short-circuit current) of irradiance sensors.

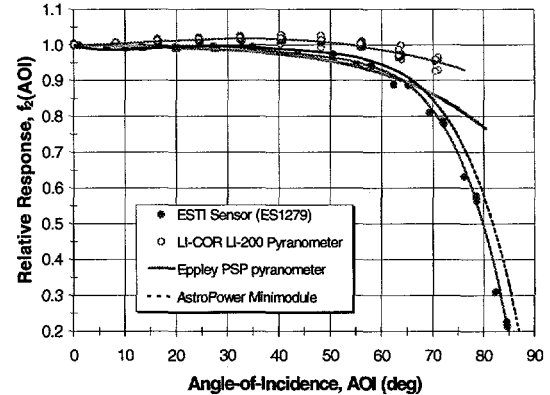


**Fig. 3:** Influence of solar angle-of-incidence (AOI) on the relative response of irradiance sensors.

## 5. OPERATING TEMPERATURE

The influence of temperature on a silicon-based irradiance sensor's response is typically small, resulting in less than 0.1 (%/°C) influence. If desired, compensation for the influence of temperature can be accomplished by determining the device temperature and applying a temperature coefficient,  $\alpha$ , which translates the measured response to a reference temperature,  $T_0$ . The temperature coefficient can be determined in the same manner routinely used for the calibration of photovoltaic reference cells [13].

Several methods can be used for determining the device temperature during operation, most of which add complexity and cost. Thermocouples can be attached to the device to directly measure the temperature. If two separate photovoltaic cells are used in the device, as in the ESTI Sensor and the AstroPower mini-module, predetermined cell parameters can be used to calculate device temperature by measuring the short-circuit current from one cell and open-circuit voltage from the other [4]. For some sensor designs, the ambient air temperature plus a small offset can be used as a reasonable estimate of the device temperature. For instance, the photodiode inside a LI-COR LI-200 pyranometer typically operates at a temperature about 6 °C above ambient temperature.

## 6. SENSOR CALIBRATION METHODS

The low-cost irradiance sensors evaluated are fundamentally photovoltaic devices, and as such, standardized test procedures can be applied to calibrate them by using a solar simulator or specific outdoor test conditions [13, 14]. By doing so, a "calibration constant,"  $C_n$ , is obtained, for one of the two standardized  $AM_a=1.5$  solar spectra, at a reference temperature,  $T_0$ . Our previous work indicated that it is also possible to separately address the spectral distribution of both the direct and diffuse components of solar irradiance [7]. However, for most practical applications of low-cost irradiance sensors, attempting to address diffuse spectral influence is probably not necessary. Standardized pyranometer calibration procedures [15, 16] can also be applied to photovoltaic irradiance sensors, as long as the  $f_1(AM_a)$  and  $f_2(AOI)$  functions are used to compensate for spectral and angle-of-incidence influences.

## 7. APPLICATION OF CORRECTIONS

Eqn. 1 gives the expression used for correcting the measured response,  $R$ , from a photovoltaic irradiance sensor for the influences of solar spectrum, angle-of-incidence, and temperature. Using the corrected response, an improved estimate for the total (broadband) irradiance,  $E_t$ , can be obtained.

$$E_t = \frac{R \cdot E_o \cdot [1 - \alpha \cdot (T - T_0)]}{C_n \cdot f_1(AM_a) \cdot f_2(AOI)} \quad (1)$$

where:

$$\begin{aligned} E_t &= \text{broadband solar irradiance, (W/m}^2\text{)} \\ R &= \text{sensor response to irradiance, (mV)} \\ E_o &= \text{reference irradiance level, 1000 (W/m}^2\text{)} \\ C_n &= \text{calibration number for device, (mV)} \\ \alpha &= \text{temperature coefficient, (1/}^{\circ}\text{C)} \\ T &= \text{device temperature, (}^{\circ}\text{C)} \\ T_0 &= \text{reference temperature, 25 (}^{\circ}\text{C)} \\ f_1(AM_a) &= \text{dimensionless polynomial} \\ f_2(AOI) &= \text{dimensionless polynomial} \end{aligned}$$

To illustrate the effectiveness of these corrections, broadband irradiance measurements using Eppley thermopile-based instruments were compared directly to the corrected measurements from the low-cost devices. Table I gives the correction parameters required for the sensors addressed in this paper. The  $A_i$  coefficients in Table I are simply the constant coefficients associated with a polynomial fit of 4<sup>th</sup> or 5<sup>th</sup> order to the  $f_1(AM_a)$  data previously shown in Fig. 2. Similarly, the  $B_i$  coefficients provide polynomial fits for the  $f_2(AOI)$  data in Fig. 3. The temperature coefficient for each device is also given in the table.

**Table I:** Coefficients required for making spectral, AOI, and temperature corrections to measurements using low-cost silicon-based irradiance sensors. Units for  $\alpha$  are (1/°C).

Coef	LICOR	LICOR w/ coll.	ESTI Sensor	API minimod
$A_0$	.932	0.933	.928	.915
$A_1$	5.401E-2	5.115E-2	6.679E-2	9.282E-2
$A_2$	-6.319E-3	-6.473E-3	-1.440E-2	-2.819E-2
$A_3$	2.631E-4	4.918E-4	1.362E-3	3.230E-3
$A_4$	0	-1.557E-5	-4.855E-5	-1.354E-4
$A_5$	0	0	0	0
$B_0$	1	N/A	1	1
$B_1$	6.074E-5	N/A	-4.849E-3	-4.281E-3
$B_2$	1.357E-5	N/A	5.447E-4	4.379E-4
$B_3$	-4.504E-7	N/A	-2.208E-5	-1.657E-5
$B_4$	0	N/A	3.709E-7	2.703E-7
$B_5$	0	N/A	-2.289E-9	-1.669E-9
$\alpha$	.00082	.00082	.00025	.00084

For clear-sky conditions, Fig. 4 graphically illustrates the result of applying the spectral and temperature corrections to global irradiance measurements using the LI-COR LI-200 pyranometer, on several different dates. On these clear days, the agreement between the LI-COR and Eppley PSP was very good, with differences less than ±3%. Without corrections, the LI-COR measurements were 10% high at low irradiance (high  $AM_a$ ) and 3% low at high irradiance (low  $AM_a$ ). Similar success has been achieved with corrections to the ESTI Sensor, the AstroPower minimodule, and the silicon reference cell.

For direct normal irradiance measurements, a LI-COR pyranometer was fitted with a plastic collimator tube. The tube was painted black on the inside, was fitted with internal baffles, and sized to provide the same acceptance angle as a typical thermopile pyrheliometer. For clear-sky conditions, the LI-COR with collimator agreed remarkably well with a secondary standard Eppley NIP pyrheliometer, within less than 0.5% over a 3-day test period. Additional testing of this device is in progress.

Overcast sky conditions and intermittent clouds present a larger challenge for all irradiance measuring devices, including thermopile pyranometers. Fig. 5 shows a comparison between the LI-COR and Eppley PSP, for overcast-sky test conditions of four different dates. The majority of corrected data agreed within less than  $\pm 5\%$ ; but without corrections, differences ranged from 15% high to 15% low. These results indicated that even though the spectral and optical issues associated with overcast conditions are complex, reasonably accurate irradiance measurements can be achieved with low-cost devices.

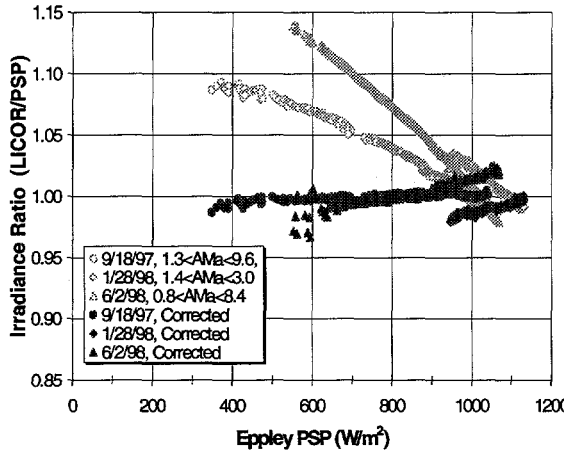


Fig. 4: For clear sky conditions, ratio of corrected irradiance measurements by LI-COR pyranometer to irradiance indicated by Eppley PSP thermopile pyranometer. Instruments mounted on solar tracker to eliminate AOI effects.

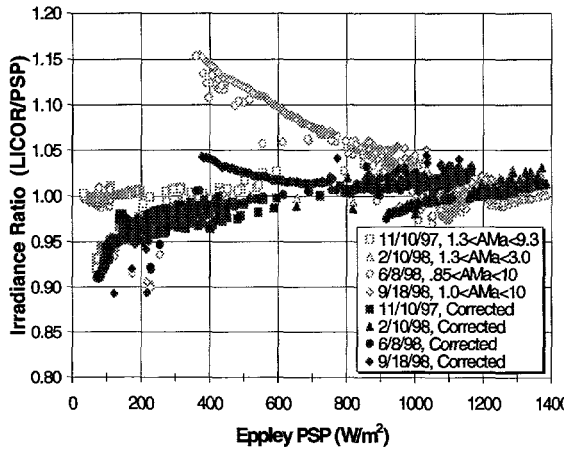


Fig. 5: For overcast sky conditions, ratio of corrected irradiance measurements by LI-COR pyranometer to irradiance indicated by Eppley PSP thermopile pyranometer. Instruments mounted on solar tracker to eliminate AOI effects.

## 8. CONCLUSIONS

By applying empirically determined corrections for the influences of solar spectrum, angle-of-incidence, and operating temperature, low-cost photovoltaic-based irradiance sensors can be used to provide accurate ( $\pm 3\%$ ) instantaneous measurements of both the global solar irradiance and the direct normal irradiance. The results of this work will enable solar system engineers to more accurately and cost-effectively evaluate the performance of their systems.

Low cost is certainly an advantage. In addition, photodiode pyranometers are small, light weight, provide the opportunity for low-cost redundancy, can be calibrated quickly with a solar simulator, provide rapid response time, and can easily be modified to measure direct normal irradiance. Two-cell sensors with planar glass covers are potentially even lower cost than photodiode pyranometers, but have more sensitivity to angle-of-incidence. If cells and mechanical design match that of a photovoltaic array, two-cell sensors can also provide an estimate of array short-circuit current and operating temperature, as well as solar irradiance.

## 9. ACKNOWLEDGEMENTS

The authors would like to acknowledge test support from Jay Kratochvil (Sandia), collimator fabrication by Don Ellibee (Sandia), radiometric consultation from Phil Thacher (Sandia), collaborative research with Daryl Myers (NREL), and industrial collaborations with John Wurm (LI-COR) and John Cummings (AstroPower).

## 10. REFERENCES

- [1] LI-COR Incorporated, [www.licor.com](http://www.licor.com).
- [2] Kipp & Zonen, [www.sci-tec.com](http://www.sci-tec.com).
- [3] ASTM E 1040, American Society for Testing and Materials Standard.
- [4] C. Helmke, W. Zaaiman, and H. Ossenbrink, 25<sup>th</sup> IEEE PVSC, 1997, pp.1267-1270.
- [5] AstroPower Incorporated, [www.astropower.com](http://www.astropower.com).
- [6] D. L. King and D. R. Myers, 26<sup>th</sup> IEEE PVSC, 1997, pp.1285-1288.
- [7] D. L. King, J. A. Kratochvil, and W. E. Boyson, 26<sup>th</sup> IEEE PVSC, 1997, pp.1113-1116.
- [8] The Eppley Laboratory Inc., [www.eppleylab.com](http://www.eppleylab.com).
- [9] ASTM E 973.
- [10] ASTM E 892.
- [11] ASTM E 891
- [12] J. Duffie and W. Beckman, *Solar Engineering of Thermal Processes*, 2<sup>nd</sup> Edition, Wiley & Sons, 1991.
- [13] ASTM E 1125.
- [14] ASTM E 948.
- [15] ASTM E 941.
- [16] ASTM E 913.